# Resonant tunneling in (110) oriented interband diodes

J. J. Zinck, D. H. Chow, K. S. Holabird, J. N. Schulman, K. C. Hall, and T. F. Boggess

Citation: Applied Physics Letters **86**, 073502 (2005); doi: 10.1063/1.1862335
View online: http://dx.doi.org/10.1063/1.1862335
View Table of Contents: http://scitation.aip.org/content/aip/journal/apl/86/7?ver=pdfcov
Published by the AIP Publishing

**Articles you may be interested in**

Influence of InGaN sub-quantum-well on performance of InAlN/GaN/InAlN resonant tunneling diodes
J. Appl. Phys. **116**, 074510 (2014); 10.1063/1.4893561

Reproducibility in the negative differential resistance characteristic of In0.17Al0.83N/GaN resonant tunneling diodes—Theoretical investigation
J. Appl. Phys. **113**, 194509 (2013); 10.1063/1.4804414

Resonance-tunneling-assisted emission enhancement in green light-emitting diodes with nanocraters formed in In Ga N ∕ Ga N quantum-well active layers
Appl. Phys. Lett. **86**, 132102 (2005); 10.1063/1.1890475

Ferromagnetic resonant interband tunneling diode
Appl. Phys. Lett. **82**, 2296 (2003); 10.1063/1.1566085

Barrier roughness effects in resonant interband tunnel diodes
J. Appl. Phys. **90**, 6177 (2001); 10.1063/1.1415539

NEW Special Topic Sections
NOW ONLINE
Lithium Niobate Properties and Applications: Reviews of Emerging Trends
AIP Applied Physics Reviews

Reuse of AIP Publishing content is subject to the terms at: https://publishing.aip.org/authors/rights-and-permissions. Download to IP: 129.173.74.49 On: Wed, 25 May 2016 12:08:48

HTML ABSTRACT + LINKS

APPLIED PHYSICS LETTERS **86**, 073502 (2005)

# Resonant tunneling in (110) oriented interband diodes

J. J. Zinck, D. H. Chow, K. S. Holabird, and J. N. Schulman
*HRL Laboratories, LLC, Malibu, California 90265*

K. C. Hall[a] and T. F. Boggess
*Department of Physics and Astronomy, University of Iowa, Iowa City, Iowa 52242*

(Received 12 October 2004; accepted 10 December 2004; published online 7 February 2005)

Growth of high-quality Sb-based resonant tunneling diodes in the (110) orientation is demonstrated. The room-temperature current–voltage characteristics of the diodes are studied as a function of GaSb well width. Electronic band structure calculations including spin support the conclusion that the position of the GaSb light hole band with respect to the InAs conduction band is responsible for the strength of the negative differential resistance observed. The spin splitting of the heavy hole band is calculated to be larger than the light hole band suggesting that the observation of negative differential resistance may not be necessary or desirable for spin transport in these structures. © *2005 American Institute of Physics*. [DOI: 10.1063/1.1862335]

Growth of quantum well devices in the (110) orientation is of interest because of applications to spintronics.[1] A quantum well structure grown in the (110) orientation offers the possibility of a longer spin lifetime than the corresponding (100) structure, because the effective magnetic field in the reference frame of a moving charge in the crystal field is polarized along the growth direction. Consequently, the D'yakonov–Perel precessional decay mechanism for spin relaxation is suppressed for the (110) growth direction.[2] Experimental evidence exists that longer spin lifetimes are indeed observed in the case of both arsenide[3] and antimonide[4] based systems grown in the (110) orientation with respect to their (100) counterparts.

[1]Resonant interband tunneling devices (RITD) in the 6.1 Å material system have been proposed as nonmagnetic semiconductor electron spin filters in both (100) and (110) oriented heterostructures,[5,6] although the design prerequisites are different. A nonmagnetic electron spin filter has two essential design criteria. First, the electron must experience an effective magnetic field to split the Kramer's degeneracy of the spin states. In nonmagnetic spin filters of (100) orientation, the degeneracy of the spin states is removed not only by bulk inversion asymmetry (BIA) but also by the Rashba effect, which is a consequence of asymmetry built into the device by design.[7] In this case, large crystal magnetic fields are produced within the plane of the heterostructures and perpendicular to the electron wave vector. These fields necessarily lead to fast precessional spin relaxation regardless of the orientation of nonequilibrium spin. In contrast, nonmagnetic spin filters of (110) orientation are designed to be symmetric, thus avoiding, in principal, Rashba fields that would cause spin precession and subsequent decay. The spin degeneracy in the (110) oriented spin filter is lifted as a consequence of bulk inversion asymmetry (BIA), which for a (110) oriented quantum well results in a crystal magnetic field oriented in the growth direction. Thus, in the (110)-oriented spin filter the growth direction is a natural quantization axis for spin, along which precessional spin relaxation is suppressed. As a second design criterion, there must be a net lateral momentum imparted to the electrons to produce a net spin polarization, which would otherwise be zero due to time reversal symmetry. In both types of spin filters, the lateral momentum can be imparted to the electron by means of a lithographically defined lateral side gate.[5,6] Fabrication of such a device has been demonstrated for the (100) orientation,[8] and application of the process to the (110) orientation is expected to be straightforward. In this letter we show that high quality growth of Sb-based RITD devices is achievable in the (110) orientation and we study the effect of GaSb well width on the presence of negative differential resistance (NDR) in the current–voltage ($I-V$) curves of such devices.

The calculated spin split electronic band structures for (110) AlSb/GaSb quantum wells with GaSb well thicknesses of 15 and 22 Å, respectively, are shown in Fig. 1. The band structures are calculated using a nonperturbative 14-band $\mathbf{k}\cdot\mathbf{p}$ nanostructure model[9] in which BIA is included to all orders of the electron wave vector. In both of these relatively narrow well structures, the effect of confinement is to move the confined light hole band (LH1) below the InAs emitter conduction band edge such that the contribution to resonant tunneling through LH1 band is minimized. The heavy hole band (HH1) which is less affected by confinement is predicted in these calculations to lie above the InAs conduction band at zero bias. The calculations show that for this structure the spin splitting is larger in the heavy hole band. However, the observation of strongly peaked negative differential resistance (NDR) is believed to be associated with tunneling through light hole states in resonant interband tunneling structures.[10] Therefore, the selection of a layer structure where strong LH-based NDR is observed may be undesirable for a spin filter device.

A series of RITDs was grown with the epilayer structure shown in Fig. 2. Growths were performed in a VG V80 III-V MBE machine equipped with shuttered EPI Group III evaporators, shuttered EPI-valved group V cracker cells, and having reflection high-energy electron diffraction and threshold photoemission as *in situ* diagnostics. Substrate temperatures were controlled by feedback from the substrate thermocouple, which was calibrated in reference to a CI Systems NTM1 optical temperature measurement system. Group III

[a]Present address: Department of Physics and Atmospheric Science, Dalhousie University, Halifax, Nova Scotia, Canada B3H 3J5

Reuse of AIP Publishing content is subject to the terms at: https://publishing.aip.org/authors/rights-and-permissions. Download to IP: 129.173.74.49 On: Wed, 25 May 2016 12:08:48

© 2005 American Institute of Physics

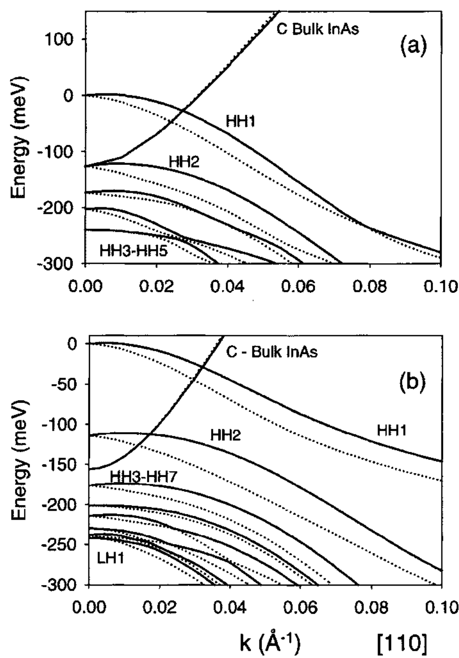


FIG. 1. Electronic band structure of an AlSb/GaSb quantum well including spin calculated with 14-band $\mathbf{k}\cdot\mathbf{p}$ nanostructure model, showing the energetic alignment of the InAs conduction band in the emitter/collector with the valence levels of the GaSb quantum well. Spin up (down) states with respect to the growth direction quantization axis are indicated by dotted (solid) lines: (a) GaSb well width=15 Å; (b) GaSb well width=22 Å.

fluxes were determined by *ex situ* x-ray diffraction measurements of calibration superlattice structures and group V fluxes were determined by *in situ* uptake measurements using threshold photoemission.[11] Gallium arsenide substrates of (110) ±0.1° orientation were obtained from WaferTech and used as received without further preparation. All substrates were subjected to a thermal oxide desorption in vacuum under group V flux. Following oxide desorption, a 1000 Å buffer of GaAs was deposited at 560 °C. The InAs $n^+$ bottom contact layer was nucleated at this temperature and then ramped at 5 °C/min to a growth temperature of 460 °C for the remainder of the structure. Top and bottom contact layers were doped with Si to $1e19$ $cc^{-1}$ and $n$-type spacer layers were doped with Si to $5e16$ $cm^{-3}$ as determined

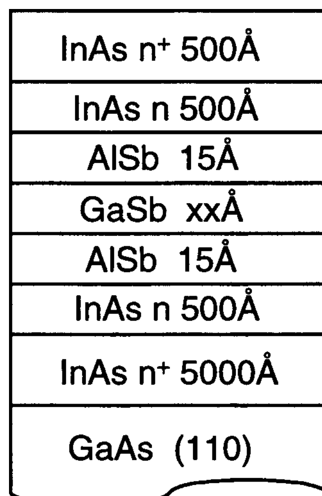


FIG. 2. Layer sequence of the InAs/AlSb/GaSb (110) RITD.

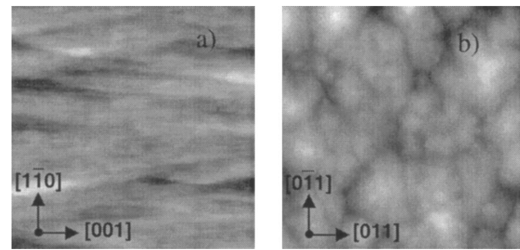


FIG. 3. AFM images of 6.1 Å heterostructures grown on (a) GaAs (110); (b) GaAs (100). Image size is 20 $\mu m^2$, measured at room temperature in air.

by independent growth and room temperature Hall measurements.

The V/III ratios during growth were typically on the order of 10:1. A characteristic of (110) growth is that a high V/III ratio, in excess of 30:1 at growth temperatures of 480 °C, is required to achieve smooth surface morphologies due to the reduced sticking coefficient of group V species on this orientation.[12] The epilayers grown in the (110) orientation in our laboratory at a V/III ratio of 10:1 exhibited a directional haze when observed under a fiber optic light, in contrast to similar structures grown in the (100) orientation, which appeared specular and featureless under the same illumination conditions. A comparison of atomic force microscopy images of identical heterostructures grown in the (100) and (110) orientations on GaAs substrates is shown in Fig. 3. The surface morphologies of these heterostructures can be reasonably assumed to be derived from the mechanisms of strain relaxation of the InAs nucleation layer on the GaAs substrate. The morphology of the (110) heteroepitaxial layer is characterized by features with preferred orientation in the (001) azimuth and are most likely associated with slip steps from the two {111} planes which intersect the (110) plane.[13] As the (100) surface has four {111} planes available for dislocation slip, no net anisotropy is expected or observed in the surface morphology. Nevertheless, at the length scale of the images, $20\times 20$ $\mu m^2$, both surfaces have a rms roughness value on the order of 2 nm, and the correspondence between a visible directional haze and successful device fabrication is not clear.

Three samples were grown with AlSb barrier thicknesses of 15 Å and GaSb well widths of 15, 20, and 25 Å, respectively. A fourth sample was grown with a 20 Å AlSb barrier and a 15 Å GaSb well. Devices were fabricated via a simple one mask process in which square Ti/Pt/Au metal features with 3, 5, and 10 $\mu$m side lengths were formed by a liftoff process. The square Ti/Pt/Au features subsequently served as a mask for a conventional wet etch to form mesas with the bottom InAs($n+$) layer as a common ground plane for all of the mesa devices. Current–voltage characteristics were acquired by probing the square mesas directly. A comparison of $I-V$ measurements for devices of dimension $5\times 5$ $\mu m^2$ are displayed in Fig. 4. In Fig. 4(a) all three RITDs have AlSb barriers of 15 Å thickness but the GaSb well thickness varies from 15 Å (solid curve) to 20 Å (dashed curve) to 25 Å (dotted curve). The device with a 25 Å GaSb well clearly exhibits NDR with a peak current of 1.4 mA and a peak-to-valley ratio of ~2. When the well width is reduced to 20 Å, although weak NDR is observed both the peak current and peak-to-valley ratio are reduced. At a well width of 15 Å NDR is no longer observed. This observation would suggest that the contribution of the light hole states to the tunneling

Reuse of AIP Publishing content is subject to the terms at: https://publishing.aip.org/authors/rights-and-permissions. Download to IP: 129.173.74.49 On: Wed, 25 May 2016 12:08:48

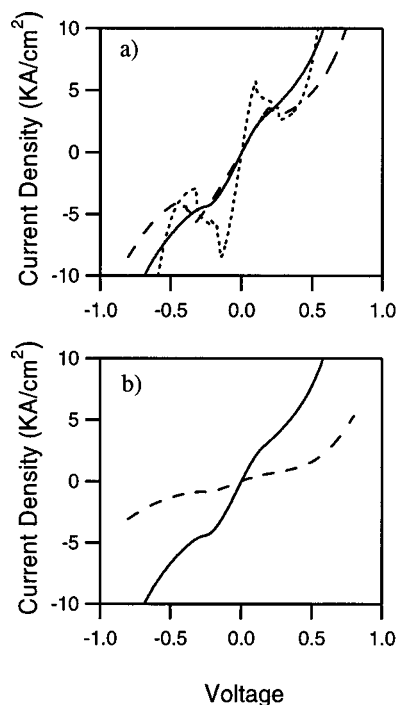


FIG. 4. Current–voltage measurements for 5 $\mu$m$^2$ (110) symmetric RITDs: (a) AlSb barrier thickness=15 Å and GaSb well thickness=25 Å (dotted curve), 20 Å (dashed curve), and 15 Å (solid curve); (b) GaSb well width =15 Å and AlSb barrier thickness=15 Å (solid curve) and 30 Å (dashed curve).

current has been minimized with this narrow well width and may be the condition desired for optimizing spin current. This is qualitatively supported by the calculated band structure of Fig. 1, where the LH1 band is ~100 meV below the InAs conduction band at zone center for a GaSb well thickness of 22 Å, but is more than 180 meV below the InAs conduction band when the GaSb well is only 15 Å thick. The coupling between the electron and HH1 state is weak and it is important to maintain a narrow barrier width to maximize tunneling current in these devices. This is illustrated in Fig. 4(b) which compares the $I-V$ measurement of two devices with 15 Å well widths but having 15 Å AlSb barriers (solid curve) and 20 Å barriers (dashed curve).

In summary, we have successfully grown symmetric RITD structures in the (110) orientation and characterized the $I-V$ characteristics of these devices at room temperature. We have correlated the thickness of the GaSb well with the observation of NDR and will use this correlation in the growth of subsequent spin filter devices to investigate the importance of heavy hole tunneling on spin filter action.

The authors wish to thank D. Ting, R. Ross, and A. Hunter for helpful discussions. This work was supported by the DARPA Spins in Semiconductors Program No. MDA972-01-C-0002. The work at the University of Iowa was also supported in part by the National Science Foundation under Grant No. ECS 03-22021 and the Natural Sciences and Engineering Research Council of Canada.

[1]S. A. Wolf, D. D. Awshcalom, R. A. Burhrman, J. M. Daughton, S. von Molnar, M. L. Roukes, A. Y. Chtchelkanova, and D. M. Treger, Science **294**, 1488 (2001).
[2]M. I. D'yakonov and V. Yu. Kachorovskii, Sov. Phys. Semicond. **20**, 110 (1986).
[3]Y. Ohno, R. Terauchi, T. Adachi, F. Matsukura, and H. Ohno, Phys. Rev. Lett. **83**, 4196 (1999).
[4]K. C. Hall, K. Gündoğdu, E. Altunkaya, W. H. Lau, M. E. Flatte, T. F. Boggess, J. J. Zinck, W. B. Barvosa-Carter, and S. L. Skeith, Phys. Rev. B **68**, 115311 (2003).
[5]D. Z.-Y. Ting and X. Cartoixa, Appl. Phys. Lett. **81**, 4198 (2002).
[6]K. C. Hall, W. H. Lau, K. Gundogdu, M. E. Flatte, and T. F. Boggess, Appl. Phys. Lett. **83**, 2937 (2003).
[7]Y. A. Bychkov and E. I. Rashba, JETP Lett. **39**, 78 (1984).
[8]J. S. Moon, D. H. Chow, D. Z. Y. Ting, J. N. Schulman, and J. J. Zinck, Appl. Phys. Lett. **85**, 678 (2004).
[9]W. H. Lau, J. T. Olesberg, and M. E. Flatte, Phys. Rev. B **64**, 161301 (2001).
[10]H. Kitabayahi, T. Waho, and M. Yamamoto, Jpn. J. Appl. Phys., Part 2 **36**, 1807 (1996).
[11]J. J. Zinck, J. H. G. Owen, and W. Barvosa-Carter, J. Vac. Sci. Technol. B **21**, 1126 (2003).
[12]E. S. Tok, J. H. Neave, M. J. Ashwin, B. A. Joyce, and T. S. Jones, J. Appl. Phys. **83**, 4160 (1998).
[13]J. G. Belk, D. W. Pashley, C. F. McConville, B. A. Joyce, and T. S. Jones, Surf. Sci. **410**, 82 (1998).

Reuse of AIP Publishing content is subject to the terms at: https://publishing.aip.org/authors/rights-and-permissions. Download to IP: 129.173.74.49 On: Wed, 25 May 2016 12:08:48